



EFFECT OF SINTERING TEMPERATURE TO MICROSTRUCTURE IN METAL BINDER JETTING

Mert GÜRGEN^{1*}, Mehmet Cengiz KAYACAN¹

¹Süleyman Demirel Üniversitesi, Mühendislik Fakültesi, Makine Mühendisliği Bölümü, Isparta, Türkiye

Keywords

*Metal binder jetting,
Additive manufacturing,
Resin,
Sintering.*

Abstract

Metal Binder Jetting emerged and it has been developing an additive manufacturing method. Binder type, binder ratio, sintering process, and atmosphere couldn't be transparently determined due to its development stage. In this study, effect of sintering temperature was investigated parts' microstructure which manufactured by Binder Jetting Metal Additive Manufacturing. In manufacturing, SS316L metal powder used as a raw material, ultraviolet light cured and solid+fluid catalyzed cured resins used as binder. For solid+liquid catalyzed cured resin, furfuryl alcohol was selected as liquid binder, para toluene sulfonic acid was selected as solid catalyst. Isopropyl alcohol was used to dilute the ultraviolet light cured resin. The composition ratios and electron diffraction patterns of the samples were analyzed using optical and scanning electron microscopy.

BAĞLAYICI PÜSKÜRTMELİ METAL EKLEMELİ İMALATTA SİNERLEME SICAKLIĞININ MİKRO İÇYAPIYA ETKİSİ

Anahtar Kelimeler

*Bağlayıcı püskürtmeli metal
eklemeli imalat,
Eklemeli imalat,
Reçine,
Sinterleme.*

Öz

Bağlayıcı Püskürtmeli Metal Eklemeli İmalat yakın zamanda ortaya çıkmış ve hala gelişmekte olan bir eklemeli imalat yöntemidir. Gelişme aşamasında olmasından dolayı net bir bağlayıcı türü, oranı, sinterleme süreci ve ortamı belirlenememiştir. Bu çalışmada Bağlayıcı Püskürtmeli Metal Eklemeli İmalat yöntemi ile imal edilmiş eklemeli imalat parçalarında, sinterleme sıcaklığının mikroiyapıya etkisi incelenmiştir. İmalat için ham madde olarak SS316L metal tozu, bağlayıcı olarak ultraviyole ışıkla ve katı+sıvı reaktiflerle kürlenmiş reçineler kullanılmıştır. Katı+sıvı kürlenmiş reçine olarak furfuryl alkol sıvı reçine, para toluen sülfonik asit katı katalizör olarak seçilmiştir. Ultraviyole ışıkla kürlenmiş reçine izopropil alkol ile seyreltilmiştir. Optik ve taramalı elektron mikroskopuyla yapılan incelemelerle kompozisyon oranları ve numunelerin elektron kırınım desenlerinin analizleri de yapılmıştır.

Alıntı / Cite

Gürgen, M., Kayacan, M.C., (2022). Effect of Sintering Temperature to Microstructure in Metal Binder Jetting, Journal of Engineering Sciences and Design, 10(4), 1389-1399.

Yazar Kimliği / Author ID (ORCID Number)

M. Gürgen, 0000-0002-0838-6564
M.C. Kayacan, 0000-0003-0993-243X

Makale Süreci / Article Process

Başvuru Tarihi / Submission Date	28.04.2022
Revizyon Tarihi / Revision Date	06.07.2022
Kabul Tarihi / Accepted Date	19.08.2022
Yayın Tarihi / Published Date	30.12.2022

1. Introduction

In these days, with the technological advances, alternative ways have begun to be sought for parts that can't be manufactured with traditional manufacturing methods. One of these non-traditional manufacturing processes is Additive Manufacturing (AM) (Gürgen and Kayacan, 2020). Unlike traditional manufacturing methods, Additive Manufacturing does not work by reducing mass or mass forming the part to be manufactured from raw material. It is a system that manufactures cross-sectional areas of parts from powder or molten raw material in layers

* İlgili yazar / Corresponding author: mertgürgen@sdu.edu.tr, +90-246-211-0804

according to a properly made design (Yalçın and Ergene, 2017). It can be classified according to the material type, the way the layers are combined and the energy source. It can be defined as the production method in which the part is manufactured as desired. This technology, which has taken names such as rapid prototyping and 3D printing, is now known as Additive Manufacturing (AM) in the literature.

AM technologies have started to come to the fore as rapid prototyping systems and has shown great development since the last half of the 20th century. AM methods including, a part is produced by adding the cross-sectional areas of the designed model on top of each other in layers, starting from a digital design file. The designed 3D digital solid model is not sent directly to the AM device. The model is first converted to the Standard Tessellation Language (STL) formatted file, which is the standard interface of the AM (Duman and Kayacan, 2016). After that, the manufacturing file is transferred to the AM device, and the manufacturing process is started. This manufacturing technique, which can be considered new, brings many benefits. The most important advantages are that it can be designed without considering any restrictions on production and thus complex parts can be created, and that there is minimal waste material, no cutting tools and forces.

In Binder Jetting (BJ), which is one of the AM types; firstly, a roller is used to spread powder material throughout the build platform. The binder material is then sprayed onto the layer, similar to inkjet printers. As a result of the spraying process, the desired geometry is obtained in two dimensions. Then the same process is repeated by passing to the next layer three-dimensional part is obtained. After the manufacturing process is finished, the part is raw form. Most of the time, post processes (coating, infiltration, etc.) are done to increase the mechanical properties. Adhesive agent (in ceramics) as coating material and bronze (in metals) as infiltration material are examples of materials used for post processes (Redwood, 2019).

In Metal Binder Jetting (MBJ), it is possible to manufacture parts by using advanced technology metals such as 316, 316L, 420, Inconel 625/718, cobalt/chromium and tungsten carbide (Exone, 2022). These materials are generally preferred in areas that require advanced engineering materials such as automotive, aerospace and defense industries. In addition to these, MBJ is preferred in special areas that require high mechanical properties and complex geometry (Mouritz, 2012).

As with other existing metal AM methods, the manufactured parts do not directly become functional in the MBJ devices. In MBJ, the first step is to manufacture low-density parts with raw strength. The mechanical properties of the part are brought to the desired level by applying various post processes. (curing, sintering, infiltration, etc.) Infiltration, which is one of these steps, is the process of infilling a metal with bronze, copper, aluminum etc. that melts at a lower temperature than the main part material to the part during sintering (Yin et al., 2007; Myers et al., 2015a; Myers et al., 2015b; Tuffile et al., 2016).

Working steps of MBJ method;

- Filling the powder feed chamber and binding material,
- Taking the powder from the feeding unit and spreading it smoothly on the build platform with the spreader mechanism,
- Spraying the binder on the necessary parts (according to the solid model geometry) of the powders,
- Curing process according to the characteristics of the sprayed binder (binders that harden in air, CO₂, ultraviolet light, temperature, etc.),
- Repeating the spreading, binder spraying and curing processes in each layer until the production is finished,
- After the manufacturing process is completed, cleaning the manufacturing parts in from unbound powders,
- By taking the manufacturing part to the furnace process; burn out the binder and sintering metal powders,
- Infiltration in the gaps remaining from the binder evaporated from the part,
- If necessary, pressure sintering [usually Hot Isostatic Pressing] as a result of processes such as the manufacture of the functional part.

2. Material and Method

2.1. Material

Materials are;

- SS316L powder,
- Photopolymer resin,

- Isopropyl alcohol,
- Para toluene sulfonic acid,
- Furfuryl alcohol

used in this study.

2.1.1. SS316 powder

Before beginning the sample manufacturing, an XRD examination of the 316L powder (with 20 – 53 μm grain sizes) was carried out and compared to the literature. The diffraction pattern of the powder analyzed in Figure 1. and in the literature in Figure 2. is given (Rokosz et al., 2015).

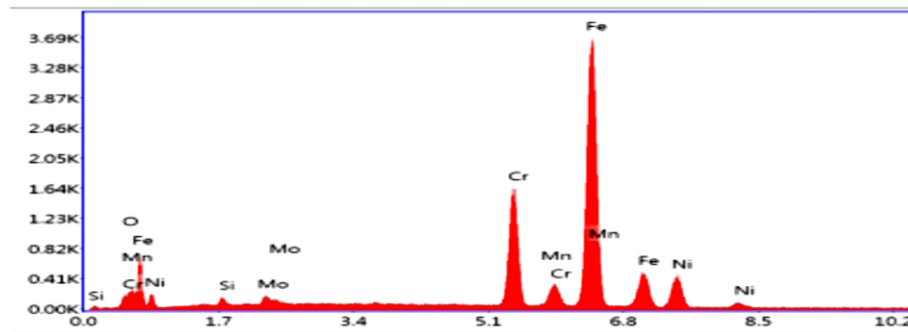


Figure 1. XRD of our study

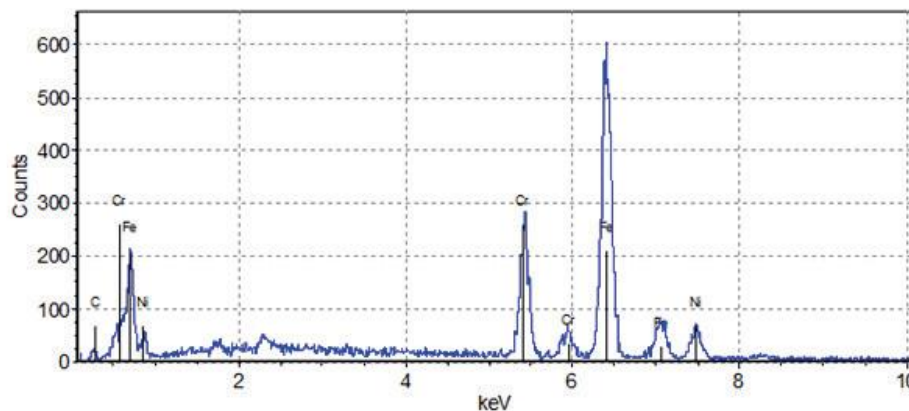


Figure 2. XRD of literature (Rokosz et al., 2015)

In Table 1., the percentages of materials are shown in comparison with the literature in terms of the powder material used. When both results were examined, it was seen that the powders were quite similar to each other, but the amount of oxygen in the powder used in the study was slightly higher.

Table 1. Composition Percentage of SS316L Powder (EOS, 2022; Renishaw, 2022)

Elements	Powder Used in Study	EOS	Renishaw
Si	0,85	0-0,75	0-1
Mo	1,5	2,25-3	2-3
Cr	17,55	17-19	16-18
Mn	2,24	0-2	0-2
Ni	11,16	13-15	10-14
C	0	0-0,03	0-0,03
S	0	0-0,01	0-0,03
P	0	0-0,025	0-0,045
N	0	0-0,1	0-0,1
Cu	0	0-0,5	0
O	1,52	0	0-0,1
Fe	Balanced	Balanced	Balanced

2.1.2. Photopolymer Resin

Photopolymer (SLA) Resin becomes polymer when light binds molecular chains together. In this way, the layers are added on top of each other and the production is made. The compositions of the resins used in the field of AM vary according to their usage areas. Standard resins can be used for visual productions, and more durable resins with ABS properties can be used for mechanical prototypes. In some model works, semi-flexible resins are preferred (3D Durak, 2022). The resin type commonly used in the SLA method was tested for the first time in the MBJ method in this study.

2.1.3. Isopropyl alcohol

Isopropyl alcohol (IPA), known by the names propan-2-ol, isopropanol or 2-propanol, is a colorless, flammable chemical with a strong odor. Its chemical formula is C_3H_8O . It dissolves IPA, ethyl cellulose, polyvinyl butyral, many oils, alkaloids and natural resins (Wikipedia, 2022a). Within the scope of the study, IPA was used to dilute the SLA resin.

2.1.4. Para toluene sulfonic acid

Para toluene sulfonic acid (p-TSA); it is a white solid chemical that is soluble in water, alcohols and other polar organic solvents. It is a strong organic acid like other sulfonic acids (Wikipedia, 2022b). In this study, p-TSA was used to act as a catalyst for the hardening of furfuryl alcohol. p-TSA powder was mixed with SS316L powder and spread on the substrate layer by layer.

2.1.5. Furfuryl alcohol

Furfuryl alcohol (FA) is a furan-containing organic compound. It cures into a resin when treated with acids, heat or catalysts. Its primary use is to be synthesized the furan resin. FA is used in cements, adhesives, coatings and casting resins (Wikipedia, 2022c). FA was used to bind the metal powders in the layers by cure with the p-TSA in this study.

2.2. Method

The methodology of the study is given at Figure 3.

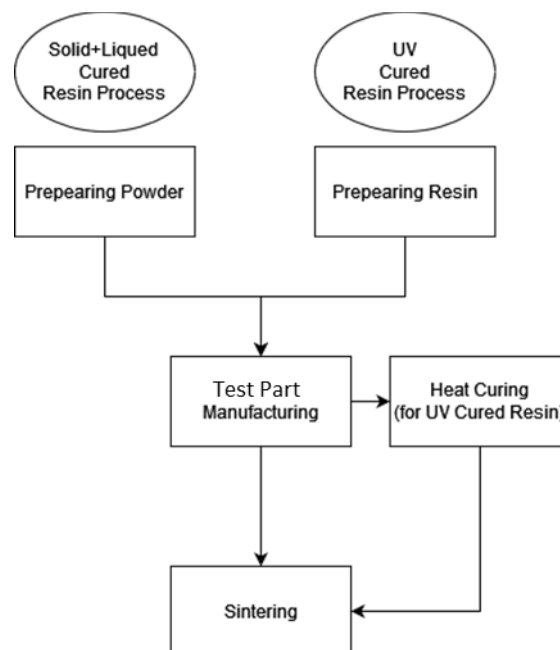


Figure 3. Diagram of methodology of the study

2.2.1. Preparing powder

Powders for solid + liquid cured manufacturing p-TSA and SS316L were mixed and made ready for manufacturing.

2.2.2. Preparing binder

SLA resin has a wettability problem when sprayed onto powders. It can't wet the powders because of the surface tension. To prevent this, SLA resin was diluted with IPA.

2.2.3. Test part manufacturing

Within the study, the samples whose mechanical properties will be examined were modeled as $\varnothing 10 \times 10$ mm cylinders as in Figure 4.

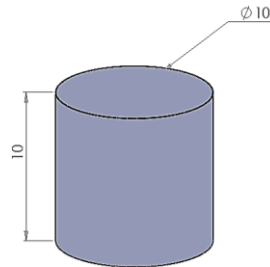


Figure 4. Test part dimensions

The powder mixture of p-TSA and 316L was laid on the fabrication table and FA was sprayed onto the layer with the spray head.

The sample in Figure 4. was also produced with SLA resin on the same bench. After SS316L powder was laid in the manufacturing area, SLA resin was sprayed according to the relevant layer geometry. The UV light source was held on the layer to cure the sprayed resin. 3D part was produced by repeating these processes.

2.2.3. Heat curing

UV curing wasn't enough for SLA resin. Because of that, test parts manufactured with SLA resin were heat cured at 175°C for 120 minutes. The large volume of the furnace required a longer curing process than literature in order to distribute the temperature homogeneously throughout the furnace (Taormina et al., 2018; Binnion et al., 2016).

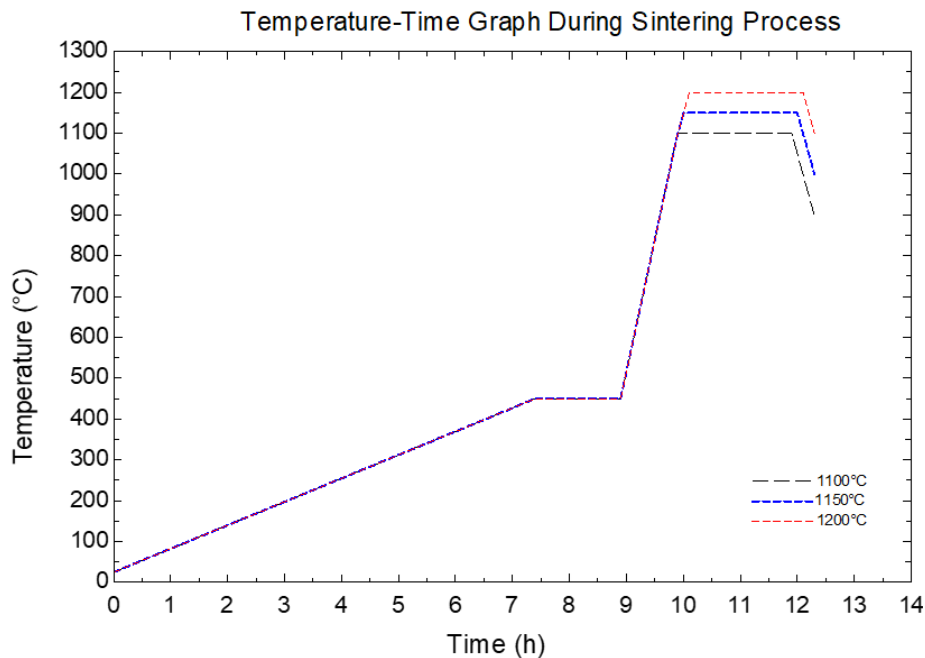
2.2.4. Sintering

The produced samples were sintered at three different temperatures (1100 , 1150 and 1200°C).

In the way of the literature;

- Inside of the furnace made nitrogen atmosphere,
- Temperature increase to 450°C with $3^{\circ}\text{C}/\text{min}$ heating rate,
- Waited at 450°C for 90 minutes,
- For make furnace vacuum atmosphere, vacuum pump was started,
- Temperature increase to sintering temperature ($1100, 1150, 1200^{\circ}\text{C}$) with $10^{\circ}\text{C}/\text{min}$ heating rate,
- Waited at sintering temperature 120 minutes,
- Waited the decreasing temperature to 150°C (by itself)

steps selected as furnace process (Vangapally et al., 2017; Johnston et al., 2004; Gülsoy, 2008; Do et al., 2017; Ren et al., 2017; Mostafaei et al., 2017; Enneti et al., 2018). Temperature-time graph during sintering process is given at Figure 5.



The initial heating rate is selected low for the best burn-out of the binder. With the same reason, waited 90 minutes at that temperature. The reason for choosing the nitrogen atmosphere is to prevent oxidation in the parts at high temperatures and to remove the burning resin vapor from the environment with nitrogen gas. With the start of the vacuum process, it is aimed to remove the resin vapor and nitrogen from the furnace atmosphere.

While the process was planned to proceed in this way, at the initial stage of the furnace process of the samples, which were planned to be sintered at 1150°C, the furnace suddenly rose to 300-350°C, then decreased to its normal values again. However, this rise burned some of the resin and prevented the samples from being sintered as desired. Another problem is that the furnace process, which is required to continue in a vacuum environment, could not create the desired furnace environment due to the lack of good vacuuming, and the resin could not be evaporated from the part.

3. Experimental Results

The internal structures of the test parts were examined in the images examined under the microscope. The structure of the powder grains and their sintering necks are shown in Figure 6. The sinter necks formed show that the process was successful and the powder grains are made neck each other, although not at the desired level.

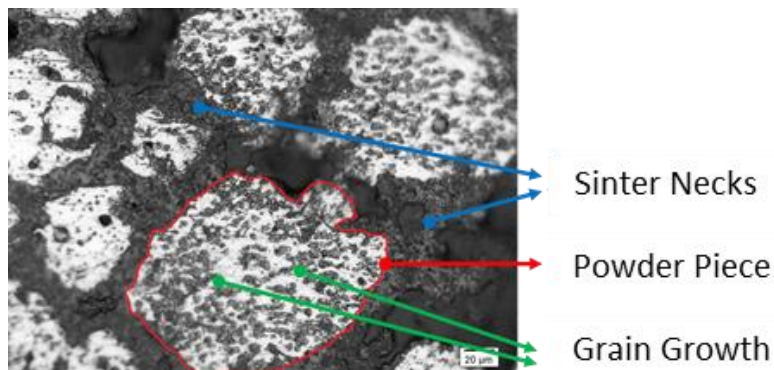


Figure 6. Microstructure of sintered sample

Figure 7. shows micro and macro pores, ferrite and austenite structures. Micro pores can be caused by the structure of the powder or for unknown reasons. Macro pores may be caused by the evaporation of the resin and the poor compaction of the powders.

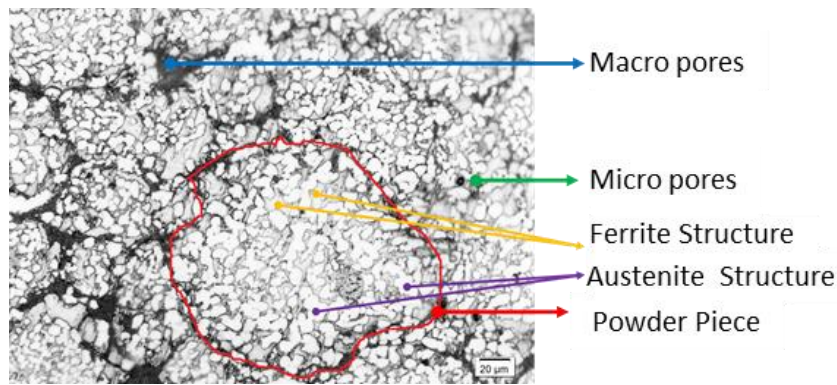


Figure 7. Etched microstructure of sintered samples

In Figure 8, ferrite and austenite structure images are given from a study in the literature (Zietala et al., 2016). Austenite cells and ferrite structures between cells can be seen in the microscope image, which is given more closely in the study.

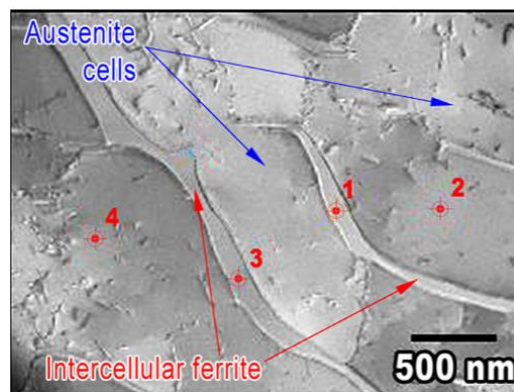


Figure 8. Etched microstructure from literature (Zietala et al., 2016)

In the atmosphere-controlled furnace environment, the nitrogen environment at first prevents the oxidation of the part. When the furnace reaches 450°C, the resin starts to burn out and mixes with nitrogen gas. After this moment, the vacuum pump is operated and the resin vapor mixed with nitrogen is removed from the environment. In cases where the vacuum cannot be done well, resin residues may remain in the part as seen in Figure 9.

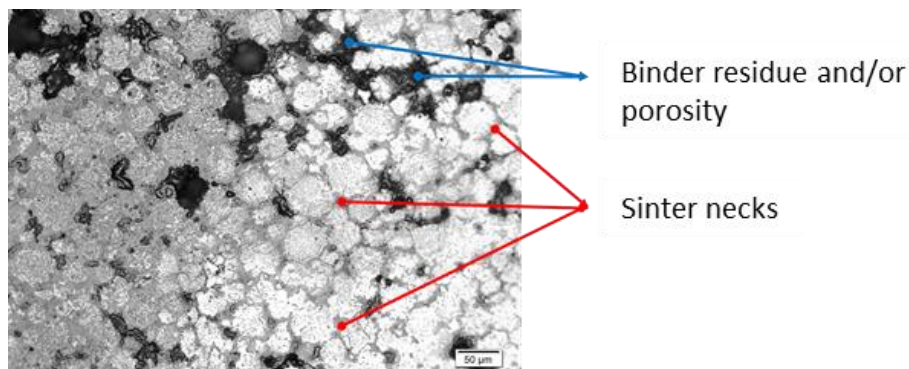


Figure 9. Porosity and binder residue at microstructure

In Figure 10., 11. and 12., the consequence of a rapid temperature rises during the heating process of the samples sintered at 1150°C is seen. While micro cracks are not visible in the samples at 1100 and 1200°C; It is quite abundant in the sample sintered at 1150°C as seen in Figure 11.

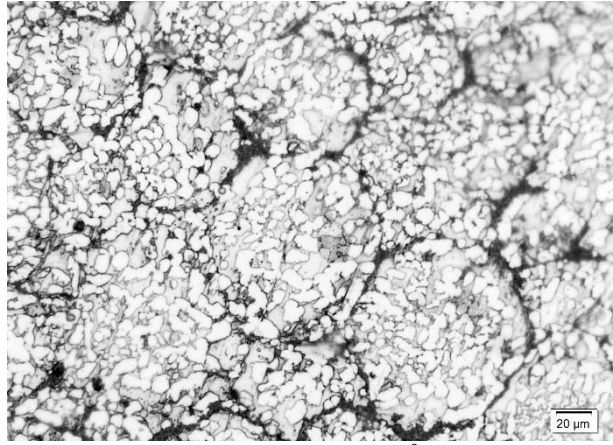


Figure 10. Microstructure at 1100°C sintered part

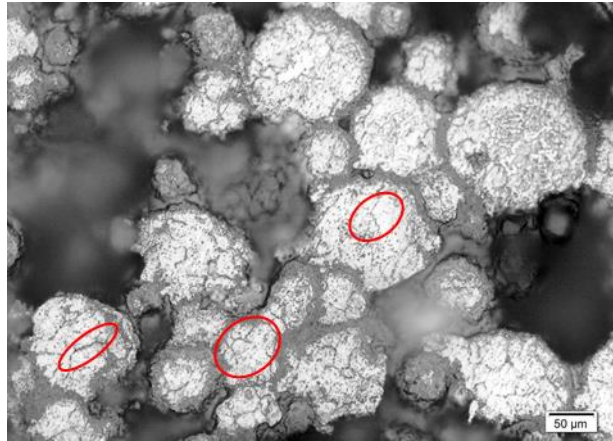


Figure 11. Microstructure at 1150°C sintered part

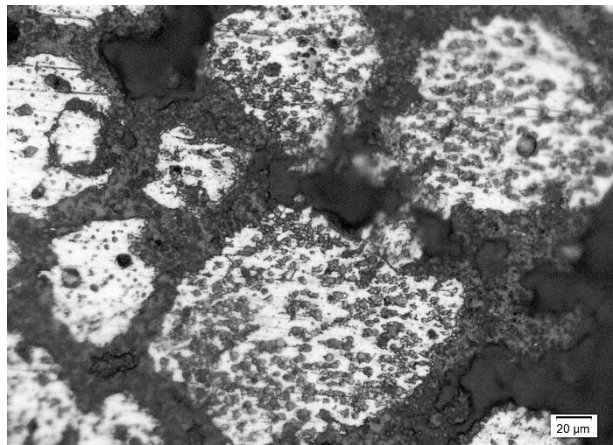


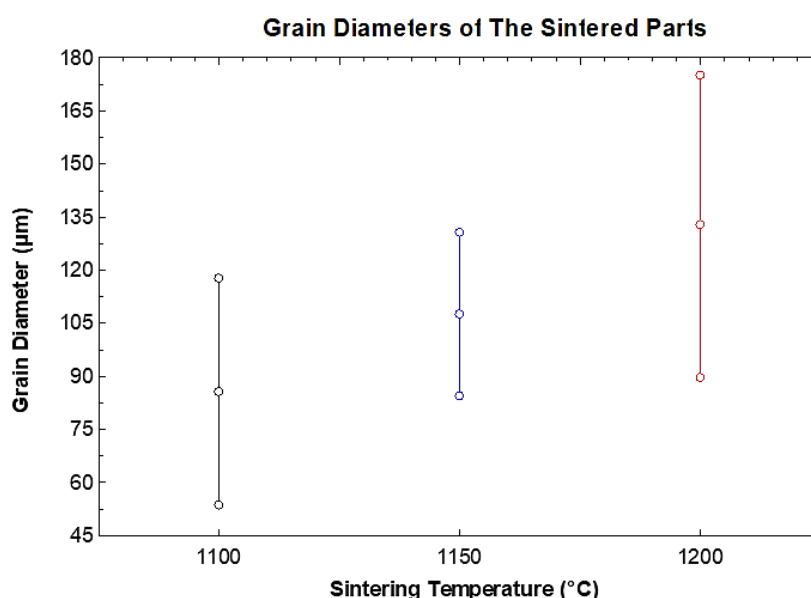
Figure 12. Microstructure at 1200°C sintered part

Grain size values according to sintering temperature and resin type are given in Table 2. The average of the measurements taken from ten grains chosen randomly was used to calculate the grain sizes.

Table 2. Grain diameters of the sintered parts

Number Of Measuring	\varnothing at 1100°C Sintering Temp. (μm)	\varnothing at 1150°C Sintering Temp. (μm)	\varnothing at 1200°C Sintering Temp. (μm)
1	53.573	84.384	89.602
2	56.060	89.899	94.081
3	57.825	91.178	124.981
4	77.907	103.355	125.331
5	79.232	107.946	148.681
6	80.769	110.147	154.090
7	84.929	121.392	159.860
8	105.820	125.276	173.710
9	111.786	127.692	174.281
10	117.648	130.605	174.991

In Figure 13. Graph of the grain diameter of the different sintering temperature.

**Figure 13.** Graph of the grain diameters of the sintered parts

In the obtained values, it was observed that the increase in the sintering temperature increased the grain sizes, similar to the literature (Stawarczyk et al., 2013; Gupta, 1972).

After sintering situation, the composition of the parts was found. At Table 3. shown the percentage of the powder which before the AM process, SLA+IPA used parts and FA+p-TSA used parts.

Table 3. EDS analysis of the sintered parts

Elements	Percentage of Powder	Percentage of SLA+IPA	Percentage of FA+p-TSA
Silicon	0,85	0,81	0,87
Molybdenum	1,5	1,33	2,98
Chromium	17,55	15,43	10,31
Manganese	2,24	2,31	0,57
Nickel	11,16	6,68	11,71
Carbon	0	12,67	5,41
Oxygen	1,52	17,05	2,95
Ferrite	Balanced	Balanced	Balanced

When the values in the table are examined, it is seen that the oxygen and carbon ratios increase as a result of sintering. The main reason for this is the non-pyrolysis binder. As a result of the burning of the binder, which cannot be removed from the part properly, at the sintering temperature, it causes the formation of oxygen and carbon waste structures in the part.

The ratio of C and O₂ among the samples produced with SLA resin is higher than those produced with p-TSA. This shows less evaporation of the resin in the part and burning residue inside the structure. The strength values of the samples decrease as the residue in the part increases.

4. Result and Discussion

Within the study, for SS316L produced by the MBJ method; the parameters related to resin type and sintering temperature were examined. It was evaluated with which parameters it gave better results in microstructure analysis.

The rapid temperature changes in heating and cooling experienced during the furnace process at 1150°C caused the formation of micro cracks in the samples. In addition, as a result of the weak vacuum process in the furnace, it causes the binder to remain in the part. This binder remaining in the part burns during sintering and causes residue.

Looking at the microstructure, it was seen that sintering between the powder grains was successful, and larger grains were formed at high temperatures. Ferrite and austenite structures in the grain were obtained. Macro and micro pores were determined. Micro pores may have been caused by a defect in the powder structure, an unknown reason. Macro pores may be the result of holes remaining from the burn out of the resins or not compacting the powders well while spreading.

For future works,

- Working with lower layer thicknesses,
- Making productions by mixing powders in different powder diameter ranges with each other,
- Sintering of samples at various temperatures,
- Trial of low resin ratios,
- Using a sintering furnace with better vacuum conditions,
- Measurement of values such as strength, density and hardness by performing HIP or infiltration on the samples,

can be recommended.

Acknowledgement

This work was supported by the Suleyman Demirel University Scientific Research Projects Coordination Unit. Project Number: FYL-2018-6709.

Conflict of Interest

No conflict of interest was declared by the authors.

References

- 3D Durak. (2022, April 18). SLA 3D Baskı Hizmeti. <https://www.3durak.com/pages/sla-3d-baski-hizmeti>.
- Binnion, J., & Arts, J. B. M. A New Method for Preparing 3D Acrylic Photopolymer Patterns for Investment Casting. In The Santa Fe Symposium on Jewelry Manufacturing Technology 2016.
- Do, T., Kwon, P., & Shin, C. S. (2017). Process development toward full-density stainless steel parts with binder jetting printing. *International Journal of Machine Tools and Manufacture*, 121, 50-60.
- Duman, B., & Kayacan, M. C. SEÇMELİ LAZER SİNERLEME TEZGÂHI İÇİN İMALAT YAZILIMI GELİŞTİRİLMESİ. *Uluslararası Teknolojik Bilimler Dergisi*, 8(3), 27-45.
- EOS. (2022, April 18). <https://www.eos.info/en>.
- Exone. (2022, April 18). <https://www.exone.com>.
- Gupta, T. K. (1972). Possible correlation between density and grain size during sintering. *Journal of the American Ceramic Society*, 55(5), 276-277.
- Gülsoy, H. Ö. (2008). Production of injection moulded 316L stainless steels reinforced with TiC (N) particles. *Materials Science and Technology*, 24(12), 1484-1491.
- GÜRGEN, M., & KAYACAN, C. BAĞLAYICI PÜSKÜRTMELİ METAL EKLEMELİ İMALATTA KULLANILAN PARAMETRELER. *Uluborlu Mesleki Bilimler Dergisi*, 3(1), 19-27.
- Johnston, S., Frame, D., Anderson, R., & Storti, D. Strain Analysis of Initial Stage Sintering of 316L SS Three Dimensionally Printed (3DP™) Components.
- Mostafaei, A., Toman, J., Stevens, E. L., Hughes, E. T., Krimer, Y. L., & Chmielus, M. (2017). Microstructural evolution and mechanical properties of differently heat-treated binder jet printed samples from gas-and water-atomized alloy 625 powders. *Acta Materialia*, 124, 280-289.
- Mouritz, A. P. (2012). *Introduction to aerospace materials*. Elsevier.
- Myers, K., Cortes, P., Conner, B., Wagner, T., Hetzel, B., & Peters, K. M. (2015). Structure property relationship of metal matrix syntactic foams manufactured by a binder jet printing process. *Additive Manufacturing*, 5, 54-59.

- Myers, K., Juhasz, M., Cortes, P., & Conner, B. (2015). Mechanical modeling based on numerical homogenization of an Al₂O₃/Al composite manufactured via binder jet printing. *Computational Materials Science*, 108, 128-135.
- Redwood, B., 2019. (2022, April 18). Additive Manufacturing Technologies: An Overview. <https://www.3dhubs.com/knowledge-base/additive-manufacturing-technologies-overview>.
- Ren, L., Zhou, X., Song, Z., Zhao, C., Liu, Q., Xue, J., & Li, X. (2017). Process parameter optimization of extrusion-based 3D metal printing utilizing PW-LDPE-SA binder system. *Materials*, 10(3), 305.
- Renishaw. (2022, April 18). <https://www.renishaw.com/en/data-sheets-additive-manufacturing--17862>.
- Rokosz, K., Hryniewicz, T., Raaen, S., & Valiček, J. (2015). SEM/EDX, XPS, corrosion and surface roughness characterization of AISI 316L SS after electrochemical treatment in concentrated HNO₃. *Tehnički vjesnik*, 22(1), 125-131.
- Stawarczyk, B., Özcan, M., Hallmann, L., Ender, A., Mehl, A., & Hämmerlet, C. H. (2013). The effect of zirconia sintering temperature on flexural strength, grain size, and contrast ratio. *Clinical oral investigations*, 17(1), 269-274.
- Taormina, G., Sciancalepore, C., Bondioli, F., & Messori, M. (2018). Special resins for stereolithography: In situ generation of silver nanoparticles. *Polymers*, 10(2), 212.
- Tuffile, C. D., Lemke, H., & Mack, P. E. (2016). U.S. Patent Application No. 15/014,637.
- Vangapally, S., Agarwal, K., Sheldon, A., & Cai, S. (2017). Effect of Lattice Design and Process Parameters on Dimensional and Mechanical Properties of Binder Jet Additively Manufactured Stainless Steel 316 for Bone Scaffolds. *Procedia Manufacturing*, 10, 750-759.
- Wikipedia, 2022a. (2022, April 18). Isopropyl Alcohol. https://en.wikipedia.org/wiki/Isopropyl_alcohol.
- Wikipedia, 2022b. (2022, April 18). P-toluenesulfonic Acid. https://en.wikipedia.org/wiki/P-Toluenesulfonic_acid.
- Wikipedia, 2022c. (2022, April 18). Furfuryl Alcohol. https://en.wikipedia.org/wiki/Furfuryl_alcohol.
- YALÇIN, B., & Ergene, B. (2017). ENDÜSTRİDE YENİ EĞİLİM OLAN 3-B EKLEMELİ İMALAT YÖNTEMİ VE METALURJİSİ. *SDU International Journal of Technological Science*, 9(3)
- Yin, X., Travitzky, N., & Greil, P. (2007). Near-Net-Shape Fabrication of Ti₃AlC₂-Based Composites. *International journal of applied ceramic technology*, 4(2), 184-190.
- Zhang, H., Liu, B., 2009. A New Genetic Algorithm for Order-Picking of Irregular Warehouse. *International Conference on Environmental Science and Information Application Technology*, 1, 121-124.
- Ziętala, M., Durejko, T., Polański, M., Kunce, I., Płociński, T., Zieliński, W., ... & Bojar, Z. (2016). The microstructure, mechanical properties and corrosion resistance of 316 L stainless steel fabricated using laser engineered net shaping. *Materials Science and Engineering: A*, 677, 1-10.